Preliminary research report

Dmitry Rogatkin*, Vyacheslav Shumskiy, Sergey Tereshenko and Pavel Polyakov

Laser-based non-invasive spectrophotometry – An overview of possible medical applications

Laser-basierte, nicht-invasive Spektralphotometrie – Übersicht über mögliche medizinische Anwendungen

Abstract

Background and objective: The problem of the medical application of non-invasive (*in vivo, in situ*) laser diagnostics, based on the principles of spectrophotometry and laser spectral analysis, is a topic which has recently found increasing interest in medical literature. This article presents an overview of selected studies in this field of medicine carried out in one of the oldest and largest Russian medical institutions, Moscow Regional Research and Clinical Institute (MONIKI) named after M. F. Vladimirskiy, illustrating the possible medical applications of these methods in clinical practice in different fields of medicine.
Materials and methods: The specially devised multi-functional laser diagnostic system "LAKK-M" was used as a diagnostic instrument in the majority of studies in MONIKI, allowing a combination of methods, such as non-invasive medical spectrophotometry in the form of laser fluorescence spectroscopy, laser Doppler flowmetry, tissue reflectance oximetry, etc. The system was used in both the experiments on laboratory animals, and for treatment of patients in different clinics of the institute.
Results: Within the last decade, extensive scientific data has been obtained which has opened up the possibility of using non-invasive medical spectrophotometry *i)* to diagnose disturbances in both blood microcirculation and oxygen transport in the peripheral small vessels, *ii)* to predict the results of treatment of gastro-intestinal tract ulcers and malignant oral neoplasms, *iii)* to assess the type of microcirculation and its influence on the outcome of the therapy prescribed, *iv)* to reveal imbalance in the collagen synthesis/degradation processes, and *v)* to develop techniques for monitoring pharmaceutical drug dynamics in human and animal organisms. In addition, new fundamental data have been obtained concerning the elevated accumulation of porphyrins in chronic hypoxia tissues and a rather large variability of individual physiological microhemodynamic parameters. If blood microdynamics are investigated it could lead to the future development of a new instrument for analysis of the individual features of patient's physiological condition and the pathogenesis of different diseases.
Conclusion: Methods of complex non-invasive medical spectrophotometry appear to be an efficient tool in practical medicine for differential diagnostics of a number of diseases and pathologies, as well as for monitoring and prediction of the treatment outcome. At the same time, they also create an important perspective for gaining novel and fundamental knowledge about the blood microcirculation system which was not available earlier due to the absence of the diagnostic technology allowing information to be obtained *in vivo* in real time.

Keywords: non-invasive diagnostics; fluorescence; oximetry; flowmetry; tissue.

Zusammenfassung

Hintergrund und Zielsetzung: Das Problem der medizinischen Anwendung der nicht-invasiven (*in vivo*, *in situ*) Laser-Diagnostik, die auf den Grundsätzen der Spektralphotometrie und Laser-Spektralanalyse basiert, ist zunehmend Thema in der medizinischen Literatur. Dieser Artikel gibt einen Überblick über ausgewählte Studien in diesem medizinischen Bereich, die in einer der ältesten und größten russischen medizinischen Forschungseinrichtungen – dem Moskauer Regional Research and Clinical Institute (MONIKI) – durchgeführt wurden und mögliche medizinische Anwendungen dieser Methoden in der klinischen Praxis in verschiedenen Bereichen der Medizin illustrieren.
Material und Methoden: Das speziell entwickelte multifunktionale Laser-Diagnose-System „LAKK-M" wurde als

diagnostisches Instrument in der Mehrzahl der Studien im MONIKI verwendet, so dass eine Kombination verschiedener nicht-invasiver medizinischer spektralphotometrischer Methoden (Laserfluoreszenzspektroskopie, Laser-Doppler-Flowmetrie, Oxymetrie, etc.) möglich war. Das System wurde sowohl in den Experimenten mit Versuchstieren als auch in der Behandlung von Patienten in verschiedenen Kliniken des Instituts verwendet.

Ergebnisse: Innerhalb des letzten Jahrzehnts wurden umfangreiche wissenschaftliche Daten erhoben, die die Möglichkeit eröffnet haben, die nicht-invasive medizinische Spektralphotometrie zu nutzen, um: *i*) Störungen sowohl in der Blutmikrozirkulation als auch im Sauerstofftransport in den peripheren kleinen Gefäßen zu diagnostizieren, *ii*) Behandlungsergebnisse von Magen-Darm-Geschwüren und bösartigen oralen Neubildungen vorhersagen zu können, *iii*) die Art der Mikrozirkulation und deren Einfluss auf das Behandlungsergebnis beurteilen zu können, *iv*) Ungleichgewichte in der Kollagen-Synthese bzw. in den Abbauprozessen zu offenbaren, und *v*) Techniken zur Überwachung der Wirkstoffkinetik pharmazeutischer Produkte im menschlichen und tierischen Organismus zu entwickeln. Darüber hinaus wurden neue grundlegende Daten über die erhöhte Akkumulation von Porphyrinen in chronisch mit Sauerstoff unterversorgtem Gewebe und über die große Variabilität der individuellen physiologischen mikrohämodynamischen Parameter gesammelt. Wenn die Blut-Mikrodynamik weiter untersucht wird, könnte dies in der Zukunft zur Entwicklung eines neuen Instruments zur Analyse der individuellen physiologischen Patientenparameter und der Pathogenese verschiedener Krankheiten führen.

Fazit: Methoden der komplexen nicht-invasiven medizinischen Spektralphotometrie scheinen ein effizientes Werkzeug in der praktischen Medizin für die Differentialdiagnostik von einer Reihe von Erkrankungen und Pathologien, sowie für die Überwachung und Vorhersage von Behandlungsergebnissen zu sein. Gleichzeitig schaffen sie auch eine wichtige Perspektive für die Gewinnung neuen Grundlagenwissens über die Mikrozirkulation des Blutes, das bisher wegen des Fehlens entsprechender diagnostischer Technik nicht verfügbar war, so dass Informationen *in vivo* in Echtzeit gewonnen werden können.

Schlüsselwörter: Nicht-invasive Diagnostik; Fluoreszenz; Oxymetrie; Flowmetrie; Gewebe.

***Corresponding author: Dmitry Rogatkin,** State Budgetary Organization of the Healthcare of Moscow Region, Moscow Regional Research and Clinical Institute ("MONIKI") named after

M. F. Vladimirskiy, Shepkina str. 61/2, Moscow, 129110, Russian Federation, e-mail: rogatkin@medphyslab.com
Pavel Polyakov, Vyacheslav Shumskiy and Sergey Tereshenko: State Budgetary Organization of the Healthcare of Moscow Region, Moscow Regional Research and Clinical Institute ("MONIKI") named after M. F. Vladimirskiy, Shepkina str. 61/2, Moscow, 129110, Russian Federation

1 Introduction

The problem of the medical application of non-invasive (*in vivo, in situ*) laser diagnostics, based on the principles of spectrophotometry and laser spectral analysis, is a topic which has of late found increasing interest in medical literature [1, 2]. Together with other well-known optical methods of diagnostics, such as diffuse optical tomography and optical coherence tomography [2], great expectations are currently associated with complex methods of non-invasive medical spectrophotometry (NMS) based on the simultaneous *in vivo* application of different optical diagnostic methods, such as laser fluorescence spectroscopy (LFS), laser Doppler flowmetry (LDF), tissue reflectance oximetry (TRO), pulse oximetry, etc. [3, 4]. Currently in all the large fields of medicine – surgery [5], oncology and radiology [6, 7], endoscopy [8, 9], angiology and gastroenterology [10, 11] – experimental and clinical investigations are being directed towards studying the use of NMS methods in different situations of medical practice.

All these spectrophotometry modalities use low-power (<10 mW) optical radiation, including the laser, for the *in vivo* examination of patients' organs and tissues to obtain diagnostic information about the body areas by recording backscattered, autofluorescent and/or transmitted light. Diagnosis is based on linear and quasilinear interaction of the light with optically heterogeneous and semi-transparent turbid materials and media, including the majority of human soft tissues (skin, mucosa) and liquids (blood and lymph) [2]. Under external illumination, for example, part of the radiation is immediately diffusely scattered by the skin's surface but another part penetrates the skin and reaches connective and muscular tissues, vessels, etc. This radiation undergoes multiple scattering (re-reflection) within biotissue at the borders of heterogenic anatomic and cellular structures, and partial absorbance by tissues and liquids substances, such as water, melanin, blood hemoglobin, etc. This part of the radiation, which has been weakened by multiple scattering and absorbance, emerges again at the external tissue surface, forming the so-called "backscattering flux" [3]. A small part of the radiation penetrates the organ under

study and passes completely through it, forming the transmitted flux. These fluxes can be measured by photodetectors. Various spectral components of optical radiation are absorbed and scattered differently by different biological tissues and substances. In addition, an excitation of the fluorescence within biotissues takes place. Therefore, illumination of body areas and organs with radiation of both fixed power and spectral waveband, together with the subsequent analysis of the intensity of the spectral components emerging from the tissues as a backscattered or transmitted fluxes, provide considerable relevant information about the internal structure and biochemical composition of investigated organ [3, 4].

The State Budgetary Organization of the Healthcare of Moscow Region, Moscow Regional Research and Clinical Institute ("MONIKI") was the first Russian research center in the late 1980s to give attention to this novel diagnostic method and began extensive basic research in this field of medical science [12–15]. The purpose of this article is to show possible areas of use for NMS methods in medical practice and to inform colleagues about the interesting research currently being carried out at MONIKI.

2 Multifunctional laser-based diagnostic system "LAKK-M"

The state-of-the-art NMS instrument in MONIKI today is the non-invasive multifunctional laser diagnostic system "LAKK-M". It is a result of collaboration with SPE "LAZMA" Ltd. (Moscow, Russia) and combines the best features of all the NMS diagnostic techniques mentioned in introduction. Today the vast majority of research in the NMS field is based on this system in MONIKI.

The system "LAKK-M" is a table variant of an optical electronic device connected to a computer (Figure 1) and uses the spectral waveband between 360 and 1000 nm. It contains a set of light sources with maximum wavelengths at 365 nm (LED), 532 nm (laser), 632 nm (laser), and 810 nm (laser), a self-made diffraction grating spectrometer, a set of photodetectors (photodiodes), electronic filtration schemes and signal enhancement constructed and integrated into a united system [15]. A multicore fiber-optical probe with a total diameter of maximal 2 mm is used as the main light delivery system, that enables both external examinations as well as routine intracavitary examinations using endoscopic equipment with a working channel of 2.3 mm or more in diameter. The output power at the distal end of the fiber-optical probe is about 2–3 mW for each light source. Also a standard pulse oximetric sensor

Figure 1 Non-invasive multifunctional laser diagnostic system "LAKK-M". It combines laser fluorescence diagnostics, pulse oximetry technique, laser Doppler flowmetry and tissue reflectance oximetry.

is used which is attached to the finger. "LAKK-M" provides complex spectrophotometric examinations based on all four principal NMS methods, namely 1) pulse oximetry, 2) LDF, 3) TRO, and 4) LFS [4, 15].

The software of the system determines all main system's functional capacities [16]. Based on the mass of signals and data, primarily registered in real-time with the use of improved Kubelka-Munk approach [17], it allows calculation of all principle optical characteristics of the biotissue tested in terms of the transport theory (for example, absorption coefficients) and the final transformation of this data into the medico-biological parameters (MBP) which are necessary for the physician. As primary MBP, the system "LAKK-M" enables the measurement, observation and real-time calculation of the following parameters of tissue microhemodynamics:

–   Blood perfusion index (PI) as a function of time and its mean value for the measurement period – a parameter, like blood flow, is measured in perfusional unit (pf.un.) in laser Doppler flowmetry, and indicates the red blood cells movement in tissue;

–   Functional tissue saturation of the oxyhemoglobin fraction in the mixed peripheral blood (S_tO_2) as a function of time and its mean value for the registration period;

–   Relative volume (V_b) of all hemoglobin fractions in the tissue's diagnostic volume is given as total hemoglobin, but in percentages of volume, diagnosed as a function of time and its mean value for the registration period;

–   Functional pulse saturation of the oxyhemoglobin fraction in arterial peripheral blood (S_pO_2) is measured and its mean value for the registration period.

The specific advantage of such a multifunctional diagnostic system is the opportunity to calculate complex parameters of blood microcirculation and oxygen transport within it, based on cross-calculations using the data of different diagnostic methods integrated into one system.

First of all, it includes perfusional saturation of blood oxygen calculated by the formula

$$S_tO_{2m}=S_tO_2/PI, \tag{1}$$

as well as specific oxygen uptake in the system of blood microcirculation

$$U=(S_pO_2-S_tO_2)/V_b. \tag{2}$$

Additionally, the LFS technique allows assessment of the dynamics and the levels of basic fluorescent molecules and substances accumulated within tissue (collagen, NADH, porphyrins, etc.) which may, in some respects, determine tissue biochemistry and cellular metabolism. They are estimated by the measured fluorescence spectra (Figure 2) based on the calculated coefficient of biotissue fluorescence contrast K_f:

$$K_f(\lambda_f|\lambda_e)=1+[J(\lambda_f)\cdot\beta-J_{bs}(\lambda_e)]/[J(\lambda_f)\cdot\beta+J_{bs}(\lambda_e)], \tag{3}$$

where K_f is a coefficient of fluorescence contrast ($0<K_f<2$); $J(\lambda_f)$ is a measured signal intensity in the fluorescence spectrum (λ_f); $J_{bs}(\lambda_e)$ is a measured intensity of backscattered radiation in the line of fluorescence excitation (λ_e); β is an instrumental reducing coefficient with $\beta\approx1000$ for $J_{bs}(\lambda_e)$ diminished to a level comparable with $J(\lambda_f)$.

Recently a parameter called the "transcutaneous index of substance fluorescence" or simply "fluorescence index" is used instead of Eqn. (3), which is calculated by the formula:

$$\eta(\lambda_f)_{\lambda_e}=\frac{J(\lambda_f)}{J(\lambda_f)+J_{bs}(\lambda_e)/\beta}. \tag{4}$$

provided that $\eta(\lambda_f)\lambda_e=0.5\,K_f(\lambda_f)$. With regard to the method, both these parameters are similar, but the latter translates the possible range of absolute intensities of the fluorescence of substance in the tissues into the compact interval of relative units from 0 to 1.

In general, the diagnostic system has two measurement modes – the LFS mode and the pulse oximetry-LDF-TRO mode. The accuracy of measurements for all primary measured MBP is about ±10% of the measured value [15].

The software of the "LAKK-M" system also allows the calculation of the frequency rhythms of microcirculation, management of the patients' data bases, etc. However, its additional functions are beyond the scope of this article and will be not be dealt with here.

The diagnostic system "LAKK-M" has all certificates which are required in Russia to be used in any real clinical situation. For the convenience of the patient, the special laser diagnostic cabinet was organized in MONIKI in 1995. Usually, the application of the system consists of the positioning of the fiber-optical probe on the tissue's surface to be tested and recording of all required parameters during a measuring time of several seconds or minutes. The measurement time depends on the chosen diagnostic goal.

3 Objective and methodology

The opportunities for a multifunctional diagnostic NMS system similar to "LAKK-M" for measurement of the multiple MBP mentioned above determine the field of application for these systems in medicine. The depth of the *in vivo* tissue probing is 1–2 mm for fiber-optical probes (diagnostic volume in a tissue is about 3–10 mm³) and the majority of the determined and calculated final MBP characterize the blood microcirculation and the surrounding soft tissues. The application of such systems is most effective in medical conditions associated with disturbances in microhemodynamics and biochemistry within the microcirculatory soft tissue available for study [2–4, 15].

It should be noted that disturbances of microhemodynamics in tissues and organs accompany a great number of diseases, ranging from cardiovascular to oncological [18]. Moreover, microcirculation dysfunctions often manifest themselves at early stages of many diseases at a
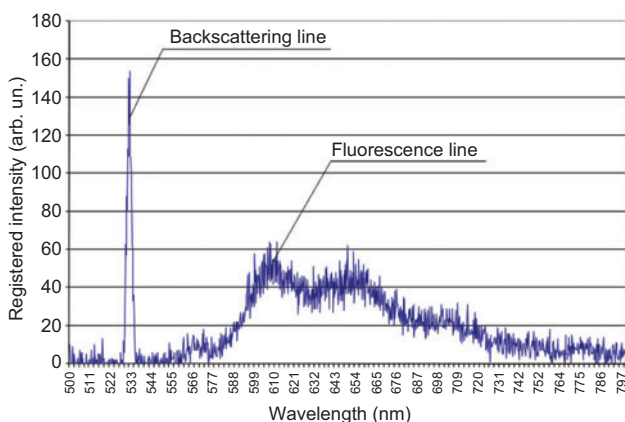

Figure 2 Typical registered fluorescent spectrum by the "LAKK-M" system. There are two main lines on the spectrum – the backscattering line and the fluorescence line. The example is for 532 nm excitation wavelength.

stage where clinical symptoms cannot yet be clearly seen. As a result it opens up unique opportunities for the early detection of many diseases. Moreover, for a series of pathologies, the perspective of a well-grounded prediction of the efficiency of medical treatment suddenly becomes apparent to the doctor. For example, early stages of ischemia and hypoxia at the level of the tissue microcirculation bed often correlate well with the final therapy outcome. In particular, a phenomenon like this was well known in the past in radiology and was named the "oxygen effect" [19–21]. According to these radiobiological prerequisites, tumors which are not well supplied with blood and oxygen are more resistant to ionizing radiation, and therefore radiotherapy is often ineffective. Fluorescence diagnostics can give additional information about dysfunction in the cellular respiratory function (cellular redox potential), disturbances in the tissue biochemistry, as well as the presence or absence of both endogenous and exogenous fluorescence markers, which is important for the differential diagnosis of a series of diseases and pathologic processes. Altogether, it has stimulated our interest in studying the information content of different NMS methods and devices for use in various fields of medicine.

4 Prediction of the therapy efficiency

4.1 Background

With regard to prediction of the therapy efficiency, the possibility to predict the likelihood of a positive therapy outcome before treatment, according to NMS data, was studied for two applications: 1) after complex medicinal and low-level laser therapy (LLLT) of long-persisting wounds of the stomach and duodenum and 2) to predict the effectiveness of radiation therapy in the treatment of head and neck cancer [7, 9, 14].

4.2 Subjects and methods

In both cases, the protocols of investigation were similar in that before treatment, all patients underwent control tests on the spectrophotometric parameters of the impaired area. For patients (n=192) with diseases of the superior gastro-intestinal tract (GIT), the center and the ulcer borders were accessible for endoscopic examination at the orthogonal fiber probe position to the tissue surface (3–4 points

with subsequent calculation of the mean values). The principal diagnostic medical parameter being assessed in this case was a coefficient of fluorescence contrast K_f for the maximum of the fluorescent signal in the area of fluorescence of endogenous porphyrins (λ_f=635–710 nm) in conditions of fluorescence excitation with a helium-neon laser (λ_e=632 nm). For head and neck tumors (17 patients), the parameters of blood microcirculation and tissue oxygenation (PI, S_tO_2, V_b) were registered from the center of the tumor (3–4 points with subsequent calculation of the mean values) and surrounding intact tissues. Then all the patients were treated according to standard protocols, i.e., a course of combined medicinal and LLLT therapy for patients with GIT diseases, and a course of radiotherapy for oncologic patients. After completion of the respective treatment courses, the results were assessed after clinical reduction of the damaged area (tumor or ulcer). For patients with GIT diseases, a 3-year follow-up study was carried out to determine the recurrence rate of the disease. Finally, all these results were compared with the spectrophotometric parameters registered before treatment, and the correlation between NMS parameters and the data of clinical observation were analyzed.

4.3 Results

4.3.1 Results of predicting the efficiency of therapy of long-persisting gastric and duodenal ulcers based on laser fluorescence spectroscopy

The group under supervision included 192 patients with a history of long-persisting ulcers: 97 patients (50.5%) with gastric and 95 (49.5%) with duodenal ulcers. In 81 patients (42.2%), the peptic ulcer was associated with gastric and duodenal erosions, in 4 patients (2.1%) with an esophageal ulcer. The main group was made up of 137 (71.4%) male patients. The patient age ranged from 18 to 80 years; 142 (74.0%) patients had a long history of peptic ulcers i.e., more than 5 years. In the majority of patients, the ulcer size ranged from 5 to 15 mm. The clinical criteria used were as follows:

- positive therapy outcome was presented as ulcer epithelization immediately after the therapeutic course and an absence of disease recurrence for 3 years;
- negative therapy outcome, manifested itself as the absence of ulcer epithelization, discovery of cancer after targeted biopsy of ulcer with subsequent referral to surgical operation, and early ulcer recurrence within 3-year period of observation [9].

In the majority of patients, a clear enhanced signal of porphyrin fluorescence from the erosion/ulcer (EU) area was registered before the beginning of the treatment. The signal changed in amplitude during the therapy course, with a trend to general reduction and leveling of the K_f coefficients, both in pathologic and healthy tissues by the end of treatment for patients with positive dynamics which was interpreted as a normalization of endogenous porphyrins content in EU area. Visual endoscopic examination during therapy showed that in the case of positive dynamics, the bottom of the ulcer, as a rule, started freeing itself of necrotic masses, fibrin deposit diminished its density, and the blood circulation increased slightly. Within 6–9 days, the ulcer began to flatten, the size of the ulcerous defect increased slightly, the fibrin deposit became a little more tender and transparent, and eventually the ulcer bottom was completely cleared of necrotic masses. By day 10–14, the ulcerous lesion had freed itself of fibrin, had started filling up with granulation tissue and had diminished in size at the expense of the edge epithelization. The most active healing began from day 16 to day 21, owing to accumulation of epithelium and formation of a tender, reddish scar or regenerator which didn't differ further from the normal mucosa. The aforementioned character of healing was shown in ~71% of patients cured of gastro-duodenal ulcers. In the rest of the 29% of patients, ulcers were repaired by the epithelial mucosal type when subsequent formation of scars in the location of ulcer was excluded. This technique of combined medication and laser effect allowed a positive outcome to be achieved in 59 patients with gastric ulcers and 61 patients with duodenal ulcers. In 36 patients with high initial K_f values, a further multiple and targeted biopsy in the area of increased fluorescence contrast revealed morphologically gastro-intestinal cancer, and these patients were referred for surgical treatment.

To assess the prognostic significance of LFS in treatment of gastro-intestinal ulcers, depending on the initial K_f values, the total number of patients was divided into 6 groups on the basis of their initial (before treatment) K_f values with following steps of the values: <0.2; 0.2–0.3; 0.3–0.4; 0.4–0.5; 0.5–0.6; and >0,6. Then the K_f-associated results in the groups were compared with the results of the clinical follow-up (Figure 3). As the diagram shows, the therapy was the most efficient in patients with an initially low K_f. It was found that if $K_f<0.2$, the efficiency of the treatment was at a maximum. The number of patients in this group with positive dynamics of gastro-intestinal ulcer repair accounted for more than 80% and with the negative dynamics, <20% (the ratio 4:1). When $K_f=0.2–0.3$, the ratio for patients with
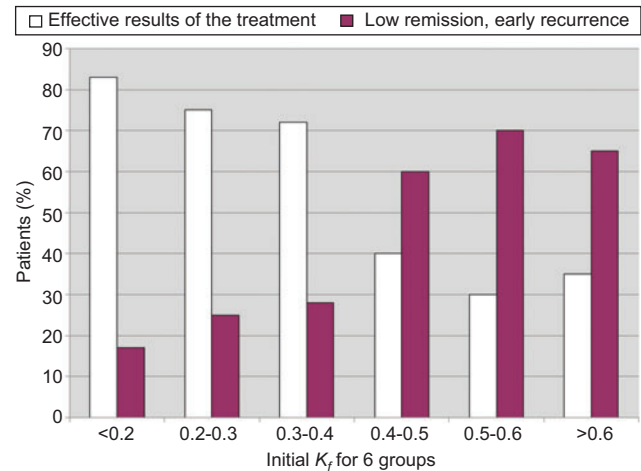

Figure 3 Efficacy of the treatment of ulcers versus initial K_f values of porphyrin fluorescence in six groups of patients. White columns represent the number of patients with good treatment results. The lower the registered initial K_f values, the better the therapy outcome.

positive and negative dynamics was already 3:1, and if $K_f=0.4–0.5$, the ratio was 2:3, i.e., the number of patients with negative outcome started prevailing over those with a positive one. In other words, the probability of the positive outcome in treatment of EU pathology with the method chosen depends on the initial level of endogenous porphyrins in the ulcer tissue. The less porphyrins that have accumulated in the lesion before treatment, the greater the probability of the positive therapy outcome. In future, it may become a patho-genetic rationale for the pre-treatment evaluation of the individual therapy regimen selected.

4.3.2 Prognosis of the efficiency of radiation treatment of the oropharyngeal zone cancer based on Doppler flowmetry and tissue reflectance oximetry data

A total of 17 patients with cancer of the oral organs (tongue, larynx, etc.) and mucosa, admitted to the MONIKI Radiologic Department, were included in the investigation. All parameters of microcirculation were registered and calculated simultaneously in real time. The mass of continuous data was processed into graphs of dependence against time, for example, $PI=PI(t)$. However, in the present investigation, for the purposes of data processing parameter values were used, measured for about 20 s. This is the maximum time possible to confidently register oral tumor parameters without

artifacts. More prolonged measurements, although more desirable and reliable, appeared to be difficult to perform in the oral cavity. Voluntary movements of the head, tongue, etc. and patient's respiration process does not allow the physician to fix a fiber-optical probe on the tumor surface for longer than 25–30 s. The parameters were recorded for each patient before the radiation course from the visible center of the tumor and from surrounding intact tissues. At the final stage of the study, in addition to the microcirculation parameters mentioned in chapter 2, and based on them, the mean value of the novel cross-calculated parameter – the index of the cellular metabolism activity (MA) – was determined for each patient giving a multiplicative integral index of oxygen metabolism in the tissues:

$$MA = U \cdot S_t O_{2m}. \tag{5}$$

The spectrophotometry parametric data for blood microcirculation and tissue respiration in tumors and intact tissues, as was obtained for each patient, are presented in Tables 1 and 2. Comparative analysis of the data obtained and data of the clinical assessment of the nearest results, i.e., results immediately after the course of ionizing radiation/chemoradiation treatment (related residual tumor volume in percentages, assessed by conventional computer tomography) showed that there was no direct correlation between the mean values of microcirculation parameters in the tumor such as PI, $S_t O_2$, V_b, $S_t O_{2m}$, U, and the treatment outcome. However, when introducing the diagnostic criterion (DC) calculated by the ratio of metabolic activity of tumor and intact tissues:

$$DC = MA_{tumor}/MA_{int}, \tag{6}$$

then its value appears to be higher than 2.5 for practically all patients with a positive outcome of treatment (0% of the tumor remnant) and <2.5 for all the rest cases (one false-positive and one false-negative, 5 true positive and 10 true negative results among 17 patients of the group). It gives a sensitivity of the method of 83%, a specificity of 91% and an accuracy of 88%. These data with short characteristic details of the nearest therapy results are presented in Table 3. Thus, the data obtained, assuming their correctness even for the greater group of patients, allows one to make two important preliminary conclusions. In practical terms, the NMS modalities enable prediction of the nearest results of radiation therapy with the value of DC (see Eqn. 6) determined *in vivo* before the therapy course begins. Basically if these results are confirmed in the future, it will be possible to put a value on the criterion dividing the border of increased sensitivity "tumor/normal". It provides further support to the well-known radiobiological hypothesis that well-oxygenated tumor cells with high proliferation (cells with high MA) are more sensitive to ionizing radiation than intact cells surrounding the tumor. These preliminary data indicate that the direct positive result of treatment is most probably achieved when the metabolic activity in tumor cells exceeds that of normal cells by 2.5-fold and more.

Table 1 Parameters of microcirculation in the tumor before radiotherapy.

Patient No.						Tumor
	PI (pf. un.)	$S_t O_2$ (%)	V_b (%)	U (arb. un.)	$S_t O_{2m}$ (arb. un.)	MA (arb. un.)
1	52.25	61.56	26.91	1.43	1.18	1.68
2	13.99	37.72	17.35	3.59	2.70	9.68
3	14.42	41.57	22.50	2.60	2.88	7.49
4	29.13	43.36	22.32	2.54	1.49	3.78
5	33.48	55.71	27.92	1.59	1.66	2.64
6	71.40	66.63	24.69	1.35	0.93	1.26
7	34.46	72.79	33.42	0.81	2.11	1.72
8	52.52	52.34	23.68	2.01	1.00	2.01
9	53.12	73.50	13.19	2.01	1.38	2.78
10	46.83	86.45	22.74	0.60	1.85	1.10
11	29.63	42.99	16.31	3.50	1.45	5.07
12	26.56	54.51	20.19	2.25	2.05	4.62
13	59.42	56.86	29.81	1.45	0.96	1.38
14	17.05	54.79	21.34	2.12	3.21	6.81
15	15.00	42.86	8.99	6.36	2.86	18.16
16	35.52	54.62	16.82	2.70	1.54	4.15
17	33.95	31.59	17.60	3.89	0.93	3.62

Table 2 Microcirculation parameters in intact tissues before radiotherapy.

Patient No.						Intact tissues
	PI (pf. un.)	S_tO_2 (%)	V_b (%)	U (arb. un.)	S_tO_{2m} (arb. un.)	MA (arb. un.)
1	10.62	22.12	13.04	5.97	2.08	12.44
2	9.00	61.29	13.71	2.82	6.81	19.23
3	34.02	66.47	24.66	1.36	1.95	2.66
4	18.15	55.38	16.31	2.74	3.05	8.35
5	48.97	55.77	18.04	2.45	1.14	2.79
6	45.85	66.39	25.05	1.34	1.45	1.94
7	25.32	82.82	25.00	0.69	3.27	2.25
8	20.36	54.24	19.98	2.29	2.66	6.10
9	40.99	93.47	26.65	0.25	2.28	0.56
10	10.55	30.29	9.88	7.06	2.87	20.26
11	13.37	76.10	19.38	1.23	5.69	7.02
12	53.02	67.27	22.83	1.43	1.27	1.82
13	85.52	69.91	29.44	1.02	0.82	0.84
14	28.78	71.56	44.47	0.64	2.49	1.59
15	21.70	83.65	17.17	0.95	3.85	3.67
16	70.84	75.02	16.46	1.52	1.06	1.61
17	48.58	51.72	22.39	2.16	1.06	2.30

5 Microcirculation disorders in fingers of patients with vibration disease

5.1 Background

In the light of NMS modalities application for early diagnosis of diseases, a decision was made to study microcirculation impairments in development of vibration disease (VD) in industrial workers under the influence of local vibration [13, 22, 23]. This disease is commonly known as Raynaud's syndrome in the English medical literature. Disturbances of vessels in the finger as angiodystonic or angiospastic syndromes, together with the lesions of the distal peripheral nerves of the upper limbs, predominate in the clinical picture of VD which is induced by local vibration (pneumatic hammers, presses, riveting equipment, etc.). It is manifested as finger whitening in the cold and/or spontaneously, accompanied with a severe pain (angiospastic syndrome) and/or hyperemia and hand edema with sensation of "heat" (angiodystonic syndrome). Vascular disturbances, peripheral innervation impairment including perivascular ones, lead to trophic alterations in distal upper limbs. Trophic disorders of the tissues manifest themselves as hyperkeratosis of the palm surface of hands and fingers with multiple fissures, nail thickening, dullness, and deformations. Stable circulation disorders play a leading role in pathogenesis of trophic anomalies [13, 22]. They often lead to disability of workers, and early detection of these disorders is important from a social point of view.

Table 3 Correlation of DC values and nearest results of the treatment.

Patient no.	Residual volume of the tumor (%)	DC
1	30	0.14
2	30	0.50
3	0	2.82
4	15	0.45
5	0	0.95[a]
6	50	0.65
7	15	0.77
8	20	0.33
9	0	4.98
10	70	0.05
11	50	0.72
12	0	2.54
13	70	1.66
14	15	4.28[b]
15	0	4.95
16	0	2.58
17	50	1.58

[a]False-negative result; [b]False-positive result.

5.2 Subjects and methods

The LDF method was used to assess the functional condition of the blood microcirculation in the workers' fingers.

The blood perfusion index *PI* was registered during the occlusion test with the patient in a sitting position and the patient's hand at the heart level. The fiber-optical sensor of the device was put on the palm surface of the distal phalanx of the right hand, 3rd finger (in the area of the close contact with vibration). Arterial occlusion was performed on the shoulder applying pressure of up to 300 mm Hg using the standard cuff of the sphygmomanometer. Shoulder arterial occlusion lasted for 2 min. The circulation was recorded continuously for 1 min before the occlusion began, during arterial occlusion, and for 2 min after occlusion termination. The mean values of *PI* before beginning with occlusion, the time taken to reaching the maximum post-occlusion reactive hyperemia, and the PI_{max} value at the moment of maximum of tissue perfusion with blood were determined. According to PI_{max}/PI ratio, at the final stage of measurement of the experimental results, the percentage of the blood flow reserve (*BFR*) was estimated to be

$$BFR = 100\% \cdot PI_{max}/PI. \qquad (7)$$

The subjects under examination were 80 men aged 37–60 years with VD and 15 healthy men of the control group with normocirculatory type of microhemodynamics. Table 4 presents data on the rate of major clinical syndromes manifesting VD in the patients examined. Vascular disturbances were the most frequent VD manifestations. In 73 (91.3%) patients, they appeared as peripheral angiodystonic or angiospastic syndromes; in 72 (90%) as a vegetosensory polyneuropathy. The stage-I VD was diagnosed in 26 (32.5%) patients. As a rule, myodystrophic and osteodystrophic syndromes are absent in stage-I VD. In 54 (67.5%) patients, the stage-II VD was found with trophic disturbances of tissues.

5.3 Results

Figure 4A and B present the blood perfusion index *PI* recorded during occlusion of the shoulder artery. The fall

Table 4 The occurrence rate of the main clinical syndromes of VD patients examined (n=80).

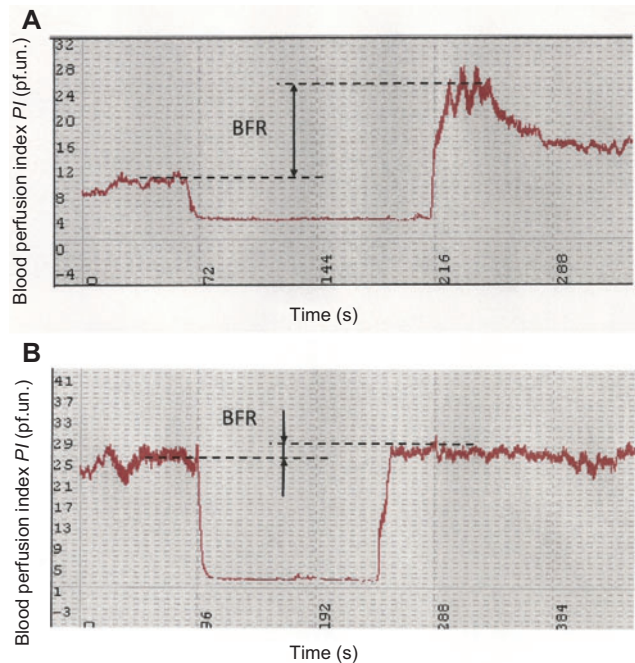| Syndrome	Syndrome occurrence rate (absolute value/%)
Peripheral angiodystonic syndrome	50 (62.5%)
Peripheral angiospastic syndrome	23 (28.8%)
Vegetosensory polyneuropathy of hands	72 (90.0%)
Myodystrophic syndrome	34 (42.5%)

Figure 4 Examples of blood perfusion indices (*PI*) measured and the blood flow reserve (*BFR*) for the occlusional test. (A) Angiospastic type of microhemodynamics. (B) Hyperemic type of microhemodynamics.

of the *PI* value indicates the beginning of the arterial occlusion, and its rise indicates the termination of the occlusion. These figures demonstrate two extreme cases of *PI* index behavior for the spastic (Figure 4A) and hyperemic types of blood microcirculation (Figure 4B). The normocirculatory type of microhemodynamics occupies the interim stage between these two extreme cases. Appearance of the reactive hyperemia (increased vascular blood supply after occlusion termination as compared to the initial occlusion level) can be explained by translation of the ischemic metabolism to anaerobic processes with vasodilator effect (synthesis of lactate and nitric oxide, and accumulation of carbonic acid). Therefore, *BFR* parameters (see Eqn. 7) assessed as blood circulation increment in the reactive hyperemia phase allows indirect estimation of the vascular endothelial function. The increased initial level of blood supply in hyperemic type of microcirculation (Figure 4B) can be indicative of the congested processes in venous circulation.

While investigating the VD groups of patients, differently directed alterations of the *PI* index were revealed. In this context, all the patients examined were additionally divided into 3 groups according to both the mean value of *PI* recorded in the minute before occlusion began and *BFR*, allocating 3 main types of blood microcirculation

Table 5 Parameters of occlusion test in VD patients and control groups.

Parameters	Group I (n=44)	Group II (n=14)	Group III (n=22)	Control (n=15)
Mean PI before test±SD (pf. un.)	8.07±2.63	22.3±6.19	12.8±3.48	15.7±3.71
PI_{max}±SD (pf. un.)	18.6±3.82	25.4±5.31	27.8±5.12	26.7±4.57
BFR±SD (%)	232.1±26.4	114.9±13.7	215.6±22.1	137.6±12.6
Time of increasing of PI_{max}±SD (s)	20.8±4.12	14.7±3.31	15.1±5.22	10.6±2.81

(normal, hyperemic and spastic types). Table 5 presents complete and statistically processed results (mean values and standard deviations, SD) of the finger occlusion test in the VD and control groups. Group I consisted of 44 (55.0%) patients with the initial mean PI value lower than that of the control group by more than 2 SD. The group II included 14 (17.5%) patients with an initial mean PI value higher than that of the control group by more than 2 SD. The group III included the rest of the patients (n=22, 27.5%) with the initial mean PI value within the control values of 2 SD.

As can be seen from the results presented here, there is an obvious and reliable ($p<0.01$) difference in BFR values between VD and control groups calculated with the use of conventional Student's t-criterion. For the VD patients, the increased time of the maximal PI_{max} amplitude growth in the reactive hyperemia phase is reliably significant. It is indicative of the potential possibility to reveal VD in the early stages using NMS methods, even in cases when the outcome differences are not so evident. It should be noted that the diagnostic procedure discussed here could be used directly in first-aid posts in the factories, usable as portable and inexpensive equipment.

6 Collagen fluorescence

6.1 Background

Another aspect of the investigations concerning differential diagnosis was associated with the assessment of cutaneous collagen and elastin fluorescence in normal and different pathologic conditions [24]. Collagen and elastin are endogenous fluorophores which account for up to 70% of the total cutaneous proteins. Therefore, they are very convenient optic markers for cutaneous structural anomalies [25, 26]. In cutaneous pathologies, such as scleroderma, basal-cell carcinoma, keloid scars, etc., the balance of collagen synthesis/degradation is impaired, so that an *in vivo* assessment of dermal collagen condition can be very promising.

6.2 Subjects and methods

In the study the endogenous fluorescence of cutaneous elastin/collagen in various skin pathologies was investigated using excitation of fluorescence by UV-LED light with a maximum wavelength of ~365 nm. Patients of the MONIKI Department of Maxillofacial Surgery who had different scars after surgical operations, basal cell cancer (BCC), and scleroderma were included in the investigation. Up to now, a total of 30 patients have been examined. The transcutaneous fluorescence indices $\eta(\lambda)_{380}$ from the pathologic area and normal intact skin were compared using the curves of $\eta(\lambda)_{380}$ plotted versus λ for every point tested. The differences were interpreted with respect to the possible non-invasive evaluation of the structural changes in the skin.

6.3 Results

The results of the examinations are presented in the Figures 5–7 as calculated transcutaneous fluorescence indices $\eta(\lambda)_{380}$ for several of our patients. As Figure 5 shows, for the 5 patients with BCC, the collagen fluorescence registered (420 nm) for the given type of dysplasia can be significantly lower than that for the intact skin (referring to intact skin of the same patient because the normal skin value was not established in these studies). To establish a normal value, large scale trials involving a significant sample of patients should be conducted with regard to gender, age, blood supply, water and melanin content in the skin, etc. Here, only individual clinical cases were observed. Nevertheless, alterations in the scar skin (Figure 6) could be seen clearly with $\eta(\lambda)_{380}$ decreasing within the whole range of λ. This situation was similar to that of BCC, and vice versa. In scleroderma (Figure 7), the fluorescence index appeared to be somewhat above its mean values for the intact skin. This result correlates well with the data in [27], according to which the balance of collagen synthesis/degradation in scleroderma shifts to a general increase in collagen synthesis.
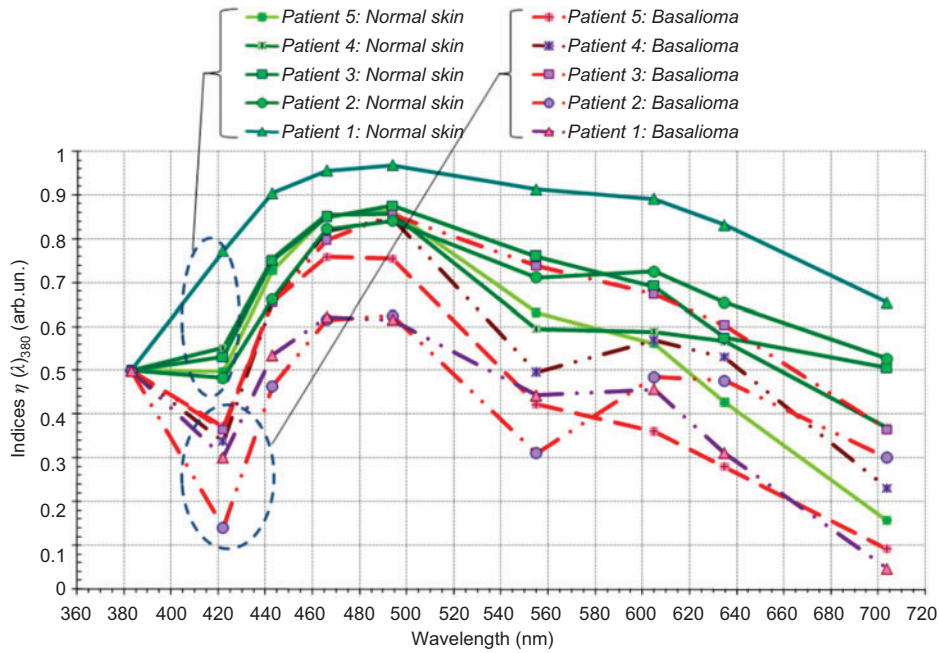
Figure 5 Indices $\eta(\lambda)_{380}$ for different tissues in patients with facial BCC. Red curves represent the area of tumor for 5 patients. Green curves represent the results for the same patients for their normal skin measured in the symmetrical side of the face.

7 Non-invasive investigation of pharmacokinetics

7.1 Background

In the past few years, another interesting and topical problem has been highlighted. It is the *in vivo* investigation of pharmacokinetics of various drug forms in human and animal organisms using NMS methods. On the one hand, it is associated with the study of new drugs produced as nano- and microcapsules which are considered promising targets for the treatment and synthesis of drugs for prolonged administration [28]. On the other hand, when the clinical testing of drugs is carried out, there is always a question as to whether a patient really took the drugs as
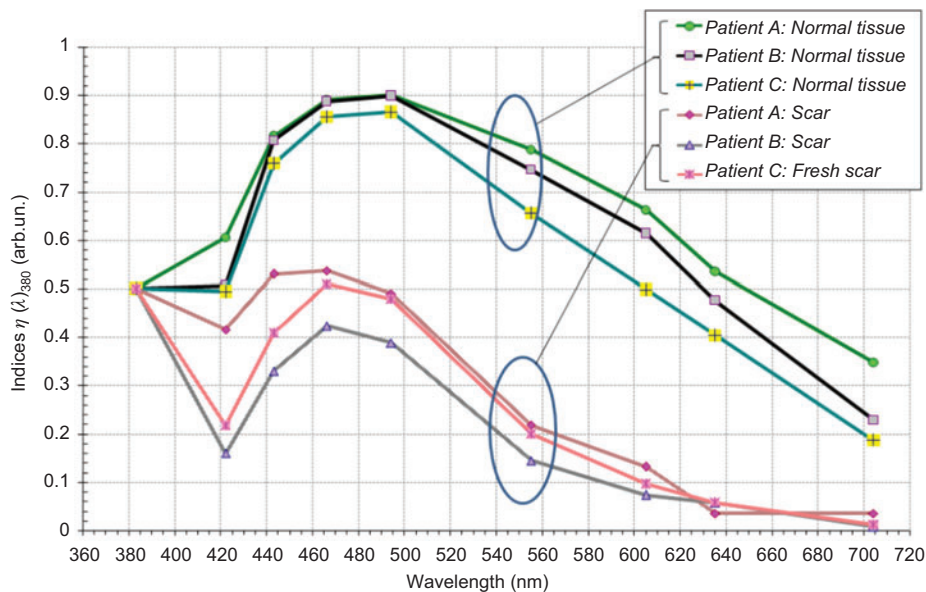

Figure 6 Indices $\eta(\lambda)_{380}$ for different tissues in patients with scars. The area of the scar and the area of the normal intact tissues were taken into account for each patient. Areas of the scar for these 3 patients have the visually low magnitudes of $\eta(\lambda)_{380}$.
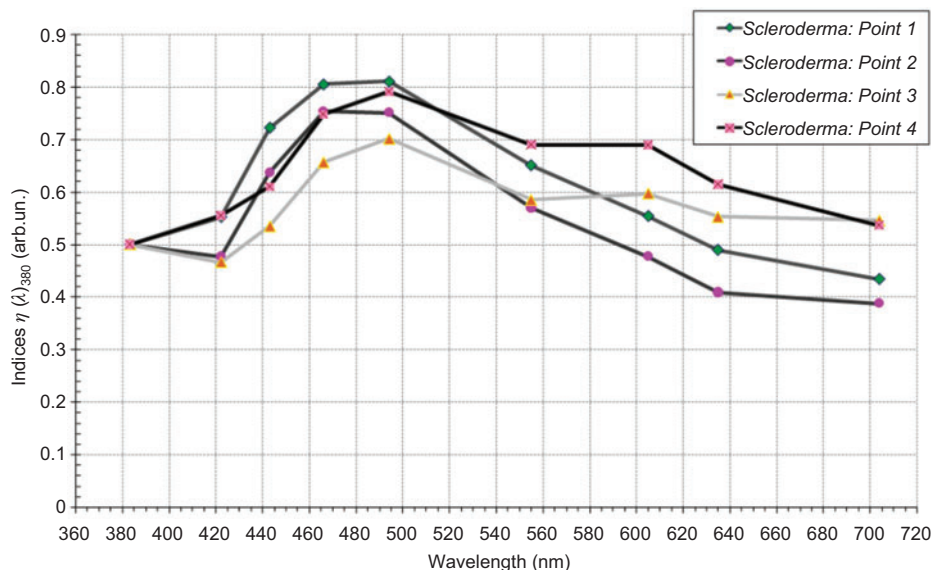
Figure 7 Indices $\eta(\lambda)_{380}$ for different tissues in a patient with scleroderma. It is apparent that these values are somewhat above the mean values for intact skin measured in other patients (for comparison see Figures 5 and 6). The patient with scleroderma has no normal intact skin.

prescribed or whether he/she secretly avoids them, does not follow the regimen or forgets to take them on time. Therefore, a non-invasive modality to monitor patient medication is an urgent necessity. For this purpose, the possibility of creating a fluorescent label on the drugs under investigation was studied enabling them to be assessed using human and animal skin fluorescence with non-invasive LFS methods. The idea of this task is similar to that of the fluorescence diagnostics in photodynamic therapy (PDT) [26] when a special exogenous fluorescent tumor marker is administered to a human organism. However these methods are significantly different. For drug taking control, in contrast to PDT procedures, the fluorescence marker should be completely non-toxic, administered orally, with easy uptake, discharge, and it should be possible for it to be measured on the surface of a healthy skin. In particular for these purposes the plant chlorophyll was considered as the fluorescent biomarker.

7.2 Subjects and methods

Investigations were performed on 20 experimental animals, non-pedigree white mice. The fundamental possibility of measuring the labeled chlorophyll *in vivo*, from the animal skin, administered orally as well as a possibility to construct a calibration curve "dose-effect" was evaluated. All mice (males, aged 6–8 months) were divided into 5 groups. One group was a control group. Four groups were given ascorbic acid (vitamin C) as the "drug" mixed

with chlorophyll extract which was added to the drinking water in different doses: 0.6 mg/kg; 4 mg/kg; 8 mg/kg; 20 mg/kg. Every day animals drank the chlorophyll solution instead of water from a dosed drinking bowl, so the uptake of chlorophyll could be easily assessed. Fluorescence was estimated by measurements of fluorescent and backscattered signal $J(\lambda)$ on the animal tail during one month experiment day by day. Before each procedure, the skin areas studied were cleaned with water and 96% ethanol. Excitation of fluorescence was performed with lasers at λ_e=532 and λ_e=632 nm.

7.3 Results

Control of the amount of water taken in gave the mean water consumption of about 70–100 ml/kg of mouse weight per day. Chlorophyll fluorescence was registered in mice skin putting the fiber-optical probe at perpendicular to the tail surface, 1 cm from its base (Figure 8), just one day after the investigation began. Chlorophyll gave the maximal fluorescent signal within the waveband λ_f=675±5 nm. It can be clearly seen from the spectra obtained that the chlorophyll signal increased with time (Figure 9) and was different for different dosages (Figure 10). In this experiment, it could be established even during the first days of regular uptake, the intensity of fluorescence in mouse skin increased and a constant concentration plateau was reached on days 6 and 7. After the end of the drug course, the fluorophore signal

Figure 8 The measuring procedure with the use of small animals and "LAKK-M" diagnostic system. Using the fiber-optical probe, the fluorescent spectrum is measured from a mouse tail.
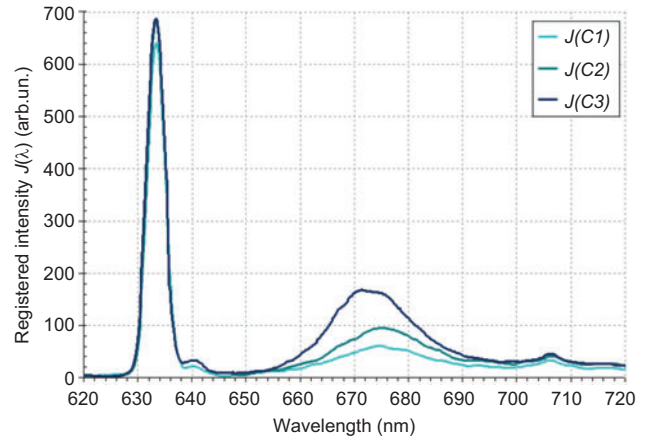

Figure 10 Correlation of the fluorescence signal $J(\lambda)$ and the chlorophyll dosage on day 7 of drug intake. $J(C1)$ – fluorophore daily dosage 0.6 mg/kg; $J(C2)$ – fluorophore daily dosage 4 mg/kg; $J(C3)$ – fluorophore daily dosage 8 mg/kg.

had almost completely disappeared by day 4. The signal intensity correlated well with the fluorophore dose enabling the construction of a calibration curve (Figure 11) that allowed the dose of the regular label uptake by fluorescence intensity to be assessed. For this purpose function $S_{J|t}$ of the relative integral mean fluorescence change within the waveband 650–690 nm was calculated by the formula:

$$S_{J|t} = \frac{1}{690-650} \int_{650}^{690} \left(\frac{J_t(\lambda_f)}{J_0(\lambda_f)} - 1 \right) d\lambda_f, \tag{8}$$

where $J_0(\lambda_f)$ is the initial spectrum of fluorescence from the control tail areas *in vivo*, before the beginning of trial; $J_t(\lambda_f)$ is a fluorescence spectrum measured at the control time t of testing with a fixed dose; and λ_f is the wavelength in nm.

Using a calibration graph, it is possible to calculate the function $S_{J|t}$ and determine the daily label dose uptake $C_J(S_J)$, from the spectral data assuming it is taken regularly. The daily dose of the concomitant pharmaceuticals, c, in mg/kg of the animal body weight was calculated with the formula:
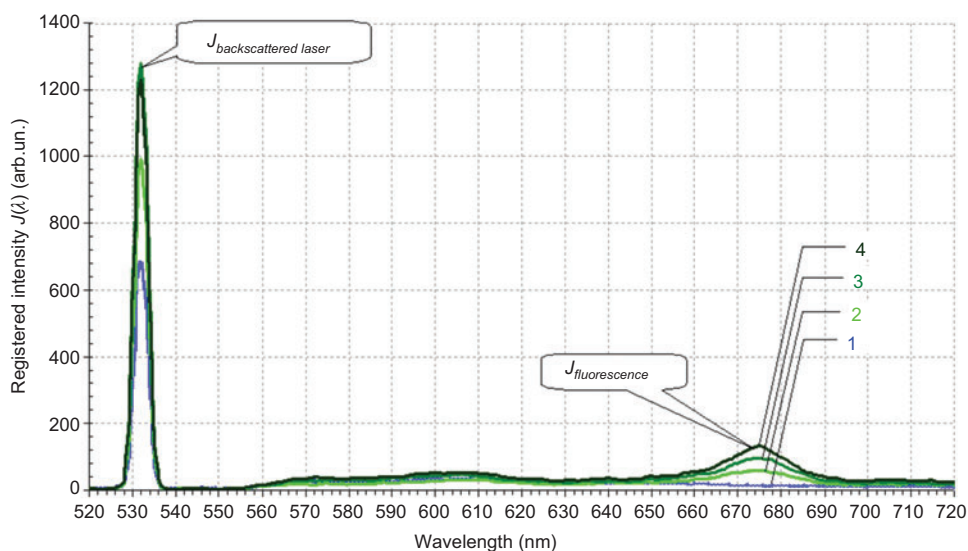

Figure 9 Correlation between fluorescence signal $J(\lambda)$ and duration of drug treatment with a daily dosage of 20 mg/kg of weight. 1 – before the beginning of drug treatment; 2 – after one day of drug treatment; 3 – after five days of drug treatment; 4 – after one month of drug treatment.
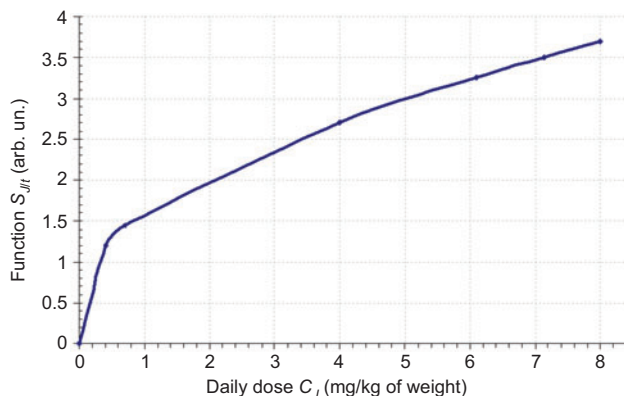
Figure 11 Calibration graph of daily label dose uptake C_J versus function S_{Jlt}. One can obtain daily label dose uptake by calculating function S_{Jlt} from the fluorescence measurement with the use of the graph.

$$c = C_J(S_J) \cdot \left(\frac{1}{\varphi} - 1 \right) = C_J(S_J) \cdot \frac{X}{F}, \qquad (9)$$

where φ is a weight-part of fluorescence label in the initial mixture. In this case, calculation of φ value was performed with regard to the ratio daily drug dose/daily label dose:

$$\varphi = \frac{F}{F + X}, \qquad (10)$$

where X (in mg/kg) is the daily dose of pharmaceuticals (vitamin C), and F (in mg/kg) is the daily dose of the fluorescent label. Thus, non-invasive fluorescent control of drug uptake is available and can be simply implemented using the LFS method.

8 Discussion

The presented data and examples show that the NMS modality opens up novel opportunities for instrumental diagnostics in medicine which as yet have not been included in other investigations in different fields of medicine. Moreover, equivalent *in vivo* information about the microcirculation of blood and the biochemical characteristics of tissue has not up to now been available to doctors or research physiologists. It can, in specific cases, establish the connection between blood microcirculation and the pathogenesis of many diseases to be regarded quite differently. In particular, the ratio of the coefficient K_f for endogenous porphyrin fluorescence in the gastro-intestinal ulcers, and the efficiency of the combined drug and laser treatment of these ulcers, raises a fundamental problem in the pathogenic substantiation of such a relationship.

Why does the efficiency of ulcer therapy decrease when accumulation of porphyrins in an ulcer is elevated? The experience of using LFS in PDT should seemingly indicate the reverse situation. In PDT, a concept is assumed that an exogenous photosensitizer, for example hematoporphyrin, quickly accumulates in fastly proliferating tumor cells. If so, in this study the quickly proliferating ulcer cells with enhanced K_f of porphyrins should lead to rapid healing of the ulcer, but just the opposite effect was obtained.

There was also an increased endogenous fluorescence in the fingers of the VD patients [13] recorded even though this disease has no connection with increased cellular proliferative activity. These results can also not be explained in the light of microbial etiology of porphyrin accumulation in cells. In general, the microbial etiology is applicable to the GIT ulcers but not applicable for patients with VD. The question is, what factor can unite all these cases? In the authors' opinion, all these results can be explained by only one factor, which is by the presence of chronic tissue hypoxia. In all the cases described here, including malignant processes, tissue hypoxia is the common and objective factor which in many respects determines the disease pathogenesis. Furthermore, the more severe the hypoxia or tissue ischemia is, the worse the effect of any drugs and physiotherapeutic procedures will be. The subsequent studies have confirmed the high probability of the correctness of this explanation [29, 30]. This in turn, opens up the possibility of a different interpretation of negative results in PDT. Photosensitizers accumulate preferably in hypoxic cells with a lack of oxygen, whereas at lower concentrations of photosynthesizer in well-oxygenated malignant cells, these cells may survive the PDT procedures. In brief, NMS also appears to be as a new and efficient instrument for fundamental research. The question is whether this can be reasonably deduced from all that has gone before?

For example, the investigations on the blood microcirculation in fingers of workers affected by VD demonstrated that about 18–20% of patients had a hyperemic type of microcirculation, and about 40% of the patients had a spastic one, which cannot as yet be explained. It is not yet known which therapeutic methods are more efficient for patients with a particular type of blood microcirculation. It is possible that some methods will be more efficient for the spastic type of microcirculation and less efficient for the hyperemic one. Hopefully at a future date it will be possible to select individual therapy tactics for each patient. For example, until now, the efficiency of the laser radiation in LLLT has often been explained by stimulation of microcirculation in the area of irradiation [31–33]. But what stimulation of microcirculation can be present in the case

of zero *BFR* for patients with hyperemic microcirculation type (Figure 4B)? Today NMS methods enable "online" measurement of the dynamics of the majority of important microcirculatory processes with very high sensitivity during any procedure. Therefore, the influence of the therapeutic factor on microcirculation can be objectively controlled. The studies show, in spite of many publications to the contrary, that stimulation of microcirculation is absent in the majority of LLLT sessions, if tissues are not heated [33], and this is true for all types of microcirculation.

Moreover, Tables 1–5 show that there is considerable individual variability among the parameters associated with blood microcirculation. It is also of note that these parameters taken on their own, without further processing, do not always have an obvious correlation with severity of the disease or the results of its treatment. This point is well-illustrated by the examples of radiotherapy of the oral cancer and by registration of microcirculation parameters in VD patients. For oral cancer none of the separate parameters in any of the single diagnostic methods correlated with results of radiotherapy. However, complex parameters of metabolic activity of the tumor cells obtained by the cross-calculation of the different NMS methods data demonstrated such a correlation. This indicates that NMS methods are the most efficient in complex, and associated applications. In the case of VD patients, a comparison between VD patients and control groups by only mean initial *PI* value, without dividing VD patients into 3 groups (Table 5) by the additional occlusion test data, did not give any significant results. The mean initial value was *PI*=11.9±3.8 for all groups of patients, and differences between them and the control group decreased due to a high value of the variability coefficient (about 32% in this case) which has not as yet been clearly explained. The additional occlusion test was only needed to reduce these variations.

Similar individual varieties can be also traced while using LFS modalities, depending also on the individual features of microhemodynamics in the area studied. Regarded from this point of view, Figure 5 is sufficiently clear. Although these 5 patients demonstrate the visual differences between pathological and normal skin collagen fluorescence, for the other measurements and their greater number, these varieties may be unreliable as was the case in a number of our measurements. However this only happens when the differences in blood supply in the areas examined weren't taken into account. It is well known that the blood hemoglobin is a strong light absorber in the waveband of collagen fluorescence and therefore it can mask the fluorescence. In this case, to obtain reliable differences between results of NMS measurements, associated application of NMS modalities and cross-calculations are necessary, including the data of LFS and TRO methods.

9 Conclusion

It can be seen that methods of the complex NMS could be efficient in public health care, both for differential diagnostics of a series of diseases and pathologies, as well as for monitoring and predicting the treatment outcome. They also create an important perspective for obtaining novel fundamental knowledge about the blood microcirculation system and the *in vivo* dynamics of tissue biochemistry. This information is now available because of advances in the relevant diagnostic technology for use in medical practice and is the reason for the interest in this research at the MONIKI. But although all NMS methods are interesting with regard to the study and application in multidisciplinary clinical and scientific research institutes, in order to obtain reliable information from the NMS methods, it is necessary to assess their complex and associated application, together with intelligent evaluation of the data. This means that for future research in this area elaboration of the corresponding interpretation algorithms is imperative.

References

[1] Johansson A, Kromer K, Sroka R, Stepp H. Clinical optical diagnostics – Status and perspectives. Med Laser Appl 2008;23(4):155–74.

[2] Tuchin VV. Handbook of optical biomedical diagnostic. Bellingham: SPIE Press; 2002.

[3] Rogatkin DA, Lapaeva LG. Prospects for development of non-invasive spectrophotometry medical diagnostics. Med Tekh 2003;37(4):217–22.

[4] Rogatkin DA, Sokolovski SG, Fedorova KA, Stewart NA, Sidorov VV, Rafailov EU. Basic principles of design and functioning of multifunctional laser diagnostic system for non-invasive medical spectrophotometry. SPIE Proc 2011;7890:78901H–78901H-7.

[5] Tseng SH, Hsu CK, Yu-Yun Lee J, Tzeng SY, Chen WR, Liaw YK. Non-invasive evaluation of collagen and hemoglobin contents and scattering property of in vivo keloid scars and normal skin

using diffuse reflectance spectroscopy: pilot study. J Biomed Opt 2012;17(7):077005.

[6] Yu G. Near-infrared diffuse correlation spectroscopy in cancer diagnosis and therapy monitoring. J Biomed Opt 2012;17(1):010901.

[7] Rogatkin DA, Polyakov PY, Bychenkov OA, Stepanenko EA. Non-invasive fluorescence diagnostics in radiotherapy of mucosal oral tumors. SPIE Proc 2002;4707:236–43.

[8] Lin K, Zheng W, Huang Z. Integrated autofluorescence endoscopic imaging and point-wise spectroscopy for real-time in vivo tissue measurements. J Biomed Opt 2010;15(4):040507.

[9] Rogatkin DA, Tereschenko SG, Lapaeva LG, Gorenkov RV. Complex therapeutic-diagnostic endoscopy with laser irradiation and in-situ spectrophotometry of erosive-ulcerative impairments of upper part of the gastrointestinal tract. SPIE Proc 2002;4613: 286–94.

[10] Jung Y, Zhi Z, Wang RK. Three-dimensional optical imaging of microvascular networks within intact lymph node in vivo. J Biomed Opt 2010;15(5):050501.

[11] Chandra M, Scheiman J, Simeone D, McKenna B, Purdy J, Mycek MA. Spectral areas and ratios classifier algorithm for pancreatic tissue classification using optical spectroscopy. J Biomed Opt 2010;15(1):010514.

[12] Dmitriev AV, Rogatkin DA, Swirin VN, Tcherkasov AS. Complex method of diagnostics of biological tissue on the basis of laser spectroscopy. Physica Medica 1999;15(3):162.

[13] Tchernyi VV, Rogatkin DA, Gorenkov RV, Karpov VN, Shumskiy VI, Lubchenko PN. Complex non-invasive spectrophotometry in examination of patients with vibration disease. SPIE Proc 2006;6078:363–70.

[14] Tchernyi VV, Rogatkin DA, Bychenkov OA, Polyakov PY. Some results of multiwave in situ autofluorescence diagnostics. SPIE Proc 2005;5693:336–43.

[15] Rogatkin DA, Lapaeva LG, Petritskaya EN, Sidorov VV, Shumskiy VI. Multifunctional laser non-invasive spectroscopic system for medical diagnostics and metrological provisions for that. SPIE Proc 2009;7368:73681Y.

[16] Rogatkin DA. Basic principles of organization of system software for multifunctional non-invasive spectrophotometric diagnostic devices and systems. Med Tekh 2004;38(2): 61–65.

[17] Rogatkin DA. A specific feature of the procedure for determination of optical properties of turbid biological tissues and media in calculation for non-invasive medical spectrophotometry. Med Tekh 2007;41(2):59–65.

[18] Tuma RF, Duran WN, Ley K, editors. Handbook of Physiology. Microcirculation. Second Edition. San Diego, Burlington, London, Amsterdam: Academic Press; 2008.

[19] Adam MF, Gabalski EC, Bloch DA, Oehlert JW, Brown JM, Elsaid AA, Pinto HA, Terris DJ. Tissue oxygen distribution in head and neck cancer patients. Head Neck 1999;21(2):146–53.

[20] Höckel M, Vaupel P. Tumor hypoxia: definitions and current clinical, biologic, and molecular aspects. J Natl Cancer Inst 2001;93(4):266–76.

[21] Osinsky S, Zavelevich M, Vaupel P. Tumor hypoxia and malignant progression. Exp Oncol 2009;31(2):80–6.

[22] Littleford RC, Khan F, Hindley MO, Ho M, Belch JJ. Microvascular abnormalities in patients with vibration white finger. QJM 1997;90(8):525–9.

[23] Bergersen TK, Hisdal J, Walløe L. Perfusion of the human finger during cold-induced vasodilatation. Am J Physiol 1999;276(3 Pt 2):R731–7.

[24] Smirnova OD, Rogatkin DA, Litvinova KS. Collagen as in vivo quantitative fluorescent biomarkers of abnormal tissue changes. J Innov Opt Health Sci 2012;5(2):1250010.

[25] Georgakoudi I, Jacobson BC, Müller MG, Sheets EE, Badizadegan K, Carr-Locke DL, Crum CP, Boone CW, Dasari RR, Van Dam J, Feld MS. NAD(P)H and collagen as in vivo quantitative fluorescent biomarkers of epithelial precancerous changes. Cancer Res 2002;62(3):682–7.

[26] Mycek MA, Pogue BW, editors. Handbook of biomedical fluorescence. New York: Marcel Dekker Inc.; 2003.

[27] Gabrielli A, Avvedimento EV, Krieg T. Scleroderma. N Engl J Med 2009;360(19):1989–2003.

[28] Preda M, Leucuta SE. Oxprenolol-loaded bioadhesive microspheres: preparation and in vitro/in vivo characterization. J Microencapsul 2003;20(6):777–89.

[29] Rogatkin DA, Bychenkov OA, Lapaeva LG. The accuracy, reliability, and interpretation of the results of in vivo laser fluorescence diagnosis in the spectral range of the fluorescence of endogenous porphyrins. Opticheskii Zhurnal 2009;76(11):708–13.

[30] Litvinova KS, Rogatkin DA, Bychenkov OA, Shumskiy VI. Chronic hypoxia as a factor of enhanced autofluorescence of endogenous porphyrins in soft biological tissues. SPIE Proc 2010;7547:75470D.

[31] Karu TI. Low-power laser therapy. In: Vo-Dinh T, editor. Biomedical Photonics Handbook. Boca Raton: CRC Press; 2002. p. 48–1.

[32] Chung H, Dai T, Sharma SK, Huang YY, Carroll JD, Hamblin MR. The nuts and bolts of low-level laser (light) therapy. Ann Biomed Eng 2012;40(2):516–33.

[33] Rogatkin DA, Shcherbakov MI, Makarov DS, Bychenkov OA. Thermal-vision monitoring of processes of heating and microcirculation of blood accompanying low-intensity laser therapeutic procedures. Opticheskii Zhurnal 2011;78(10): 666–71.